AIAA JOURNAL
Vol. 39, No. 8, August 2001

Shock Wave Control by Nonequilibrium Plasmas in Cold Supersonic Gas Flows

Samuel Merriman,* Elke Ploenjes,† Peter Palm,† and Igor V. Adamovich‡
Ohio State University, Columbus, Ohio 43210-1107

Experimental studies of shock modification in weakly ionized supersonic gas flows are discussed. In these experiments, a supersonic nonequilibrium plasma wind tunnel, which produces a highly nonequilibrium plasma flow with the low gas kinetic temperature at $M = 2$, is used. Supersonic flow is maintained at complete steady state. The flow is ionized by a high-pressure aerodynamically stabilized dc discharge in the tunnel plenum and by a transverse rf discharge in the supersonic test section. The dc discharge is primarily used for the supersonic flow visualization, whereas the rf discharge provides high electron density in the supersonic test section. High-pressure flow visualization produced by the plasma makes all features of the supersonic flow, including shocks, boundary layers, expansion waves, and wakes, clearly visible. Attached oblique shock structure on the nose of a 35-deg wedge with and without rf ionization in a $M = 2$ flow is studied in various nitrogen–helium mixtures. It is found that the use of the rf discharge increases the shock angle by 14 deg, from 99 to 113 deg, which corresponds to a Mach number reduction from $M = 2.0$ to 1.8. Time-dependent measurements of the oblique shock angle show that the time for the shock weakening by the rf plasma, as well as the shock recovery time after the plasma is turned off, is of the order of seconds. Because the flow residence time in the test section is of the order of 10 μs, this result suggests a purely thermal mechanism of shock weakening due to heating of the boundary layers and the nozzle walls by the rf discharge. Gas flow temperature measurements in the test section using infrared emission spectroscopy, with carbon monoxide as a thermometric element, are consistent with the observed shock angle change. This shows that shock weakening by the plasma is a purely thermal effect. The results demonstrate the feasibility of both sustaining uniform ionization in cold supersonic nitrogen and airflows and the use of nonequilibrium plasmas for supersonic flow control. This opens a possibility for the use of transverse stable rf discharges for magnetohydrodynamic energy extraction and/or acceleration of supersonic airflows.

I. Introduction

SHOCK wave propagation in weakly ionized plasmas (with ionization fractions of 10^{-8}–10^{-6}) has been extensively studied for the past 15 years (e.g., see Refs. 1–5 and references therein). The following anomalous effects have been observed: 1) shock acceleration, 2) nonmonotonic variation of flow parameters behind the shock front, 3) shock weakening, and 4) shock wave splitting and spreading. These effects have been observed in discharges in various gases (air, CO_2, Ar) at pressures of 3–30 torr, and for Mach numbers $M \sim 1.5$–4.5. They also persist for a long time after the discharge is off.

At the present time, no consistent theoretical model has been able to interpret the results of these studies on the basis of nonequilibrium plasma effects alone.[6] On the other hand, recent experiments in a steady-state glow discharge using spatially resolved gas temperature measurements by filtered Rayleigh scattering[7] and in pulsed glow discharge,[7] as well as modeling calculations,[8] suggest that most of these results can be explained by the nonuniform heating of the gas flow in the discharge. A major complexity with the previous experiments on the anomalous shock weakening and dispersion in nonequilibrium plasmas is that short-duration test facilities (shock tubes and ballistic ranges) have been used. A second complexity is the control of the test plasma parameters. Ideally, it is desirable to have uniform gas temperature, pressure, species concentrations, and electron density throughout the test region, and these parameters should remain constant in time. Finally, in the previous experiments the weakly ionized plasma has been produced in a stagnant or very slowly moving gas, whereas most practical applications of shock wave control by plasmas require sustaining ionization in a supersonic flow.

The present study represents an effort to address and circumvent these complexities. The present experiments are conducted in a new, unique, steady-state supersonic flow facility, with well-characterized, near-uniform, nonequilibrium plasma properties. This facility allows simultaneous measurements of the flowfield parameters (such as temperature and pressure) and electric discharge parameters (current and voltage), as well as complete supersonic flow visualization. The main objectives of the present work are to study the feasibility of the supersonic flow modification and control by nonequilibrium plasmas and to determine whether the shock weakening by plasmas reported in previous studies is indeed due to thermal effects.

II. Experimental Facility

The facility used in the present study is a recently developed, small-scale, nonequilibrium plasma wind tunnel.[9] In contrast to the shock tube and ballistic range studies, it operates at steady state. The schematic of the wind tunnel is shown in Fig. 1. The design and operation of the wind tunnel has been described in greater detail in Ref. 9. Briefly, an aerodynamically stabilized dc diffuse glow discharge in the tunnel plenum can be sustained at high pressures, up to 2/3 atm in nitrogen, or up to 6 atm in helium. This is not an arc-heated tunnel. Although the electrical power into the discharge is rather high, up to 500 W in pure N_2, more than 90% of the input power goes into the vibrational mode of nitrogen.[10] In contrast to an electric arc, very little of the power goes directly to gas heating. Therefore, conditions of the gases at the throat exhibit the extreme thermal disequilibrium of the positive column of a glow discharge; the translational/rotational mode temperature is low (~300 K for an uncooled discharge tube), the energy in the vibrational mode is high (0.1–0.2 eV per diatomic molecule), the electron density is $n_e \sim 10^{10}$ cm^{-3}, and the average electron energy is in the 1.0-eV range.

Presented as Paper 2000-2327 at the AIAA 30th Fluid Dynamics Conference, Denver, CO, 19–22 June 2000; received 11 July 2000; revision received 18 January 2001; accepted for publication 13 February 2001.

*Undergraduate Research Assistant, Nonequilibrium Thermodynamics Laboratory, Department of Mechanical Engineering.

†Postdoctoral Researcher, Nonequilibrium Thermodynamics Laboratory, Department of Mechanical Engineering.

‡Visiting Assistant Professor, Nonequilibrium Thermodynamics Laboratory, Department of Mechanical Engineering. Senior Member AIAA.

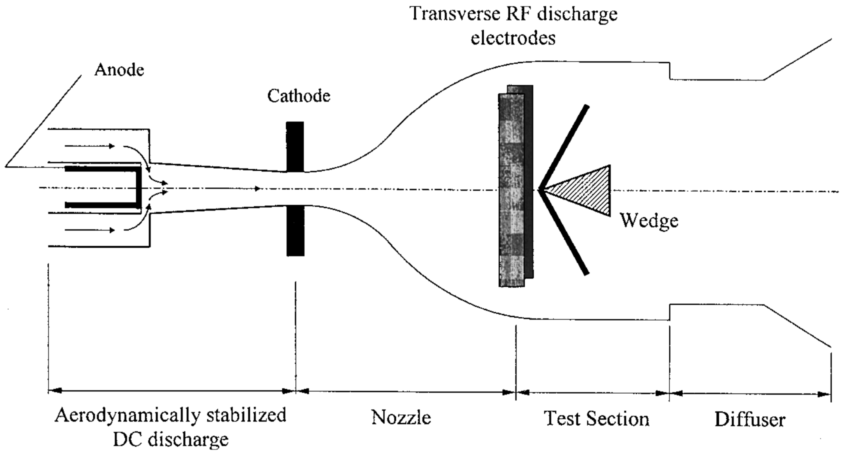

Fig. 1 Schematic of wind-tunnel experiment.

Downstream of the discharge section is a two-dimensional plane supersonic nozzle, as shown. The nozzle has a high aspect ratio of about 7.5:1, so that in the test section the nozzle width is 3 cm, whereas the distance between the top and bottom nozzle walls is 4 mm. The top and bottom walls of the nozzle are slightly diverging to provide boundary-layer relief in the third dimension. The nozzle is made of transparent acrylic plastic, with glass and CaF_2 windows, which allow optical access to the test section. Fabrication and use of a range of nozzles with varying expansion ratios and test section lengths is straightforward and rapid. The system is connected, through a simple channel diffuser, to a ballast tank pumped by a several-hundred-cubic-feet-per-minute vacuum pump. Operation at relatively high plenum pressures creates a supersonic flow, of reasonable quality (~75% inviscid core), in the test section of the tunnel.[9] At $M = 2$, run durations of at least a few minutes are attained. An important feature of the nozzle operation is that high level of vibrational excitation existing at the nozzle entrance persists throughout the nozzle length. The vibrational temperature of nitrogen is essentially frozen at the throat values. Also, the electron–ion recombination in the expansion into the test section of the tunnel is sufficiently slow, so that the ionization fraction produced in the dc discharge in the plenum ($n_e/N \sim 10^{-9}$) remains nearly constant.[9]

Our previous experiments in the $M = 3$ supersonic flowing afterglow with ionization sustained by the dc discharge in the plenum[9] did not show any measurable shock modification by the plasma. One possible reason for that was the low ionization fraction in the test section, $n_e/N \sim 10^{-9}$. In previous shock tube and ballistic range experiments, which demonstrated considerable shock dispersion and weakening,[1–5] the ionization fraction was in the range 10^{-8}–10^{-6}. In the present study, the electron density in the test section is considerably increased by using a transverse rf discharge. It is well known that rf discharges with dielectric-covered electrodes are considerably more stable than dc discharges.[10] The main reason for this is that this type of rf discharge does not form unstable high electric field cathode layers where ionization is sustained by secondary electron emission.[11] This prevents formation of cathode spots with the normal current density[10] and, therefore, allows considerable increase of the electrode surface area and the volume occupied by a uniform discharge. In the present experiment, the rf discharge is sustained between 17-mm-long, 4-mm-wide strip electrodes embedded in the top and bottom nozzle walls, as shown in Fig. 1. Both rf electrodes are covered with layers of 1–2 mm thick Pyrex® glass to prevent secondary electron emission that results in the discharge collapse into an arc. The electrodes do not extend wall to wall, which would produce considerable discharge and temperature nonuniformity in the boundary layers, because of the long flow residence time there. The rf voltage was applied to the electrodes using a 13.56-MHz, 600-W ACG-6B rf power supply and a 3-kW MFJ-949E tuner was used for rf circuit impedance matching. Typically, the reflected rf power did not exceed 5–10% of the forward power. This allowed sustaining a stable, diffuse, and uniform transverse discharge in pure nitrogen, in N_2–He mixtures, and in air. Note that initiating and sustaining of the rf discharge did not require flow preionization by the dc discharge upstream. The rms rf voltage and current were varied in the range 0.8–1.75 kV and 80–280 mA. The estimated test section electron density at these conditions is up to $n_e = 3 \times 10^{11}$ cm^{-3}, that is, two orders of magnitude higher than produced by the dc discharge, which gives an ionization fraction of $n_e/N \sim 10^{-7}$.

For the shock control studies reported here, an 8-mm-long, 35-deg plastic wedge is inserted into the supersonic ionized flow a few millimeters downstream of the rf electrodes, as shown in Fig. 1. With this system, the effect of the nonequilibrium plasmas on the strength of the resultant oblique shock attached to the nose of the wedge can be studied in detail, in a steady and well-controlled plasma environment. The objective of the experiments is to measure the oblique shock angle, under both plasma on and plasma off conditions. Previously, it has been reported that the effect of the plasma is to weaken the shock. This should produce an apparent reduction of the shock Mach number and, therefore, increase the oblique shock angle. Unlike our previous work,[9] where the shock angle was measured using a schlieren system, in the present experiments the high-pressure supersonic plasma flow visualization technique[9] is used for shock angle measurements. Because our previous experiments showed that the aerodynamically stabilized dc discharge sustained in the nozzle plenum did not produce any detectable shock angle change, in the present study this discharge is primarily used for the flow visualization. Flow images were taken using a high-resolution monochrome COHU-4910 camera and a Sony digital video camera. On the other hand, the transverse rf discharge sustained in the test section is mainly used to produce high electron densities comparable with those obtained in previous plasma shock experiments,[1–5] to study the feasibility of shock weakening by the plasma.

To determine whether the shock modification by the plasma is thermal, that is, produced by joule heating of the incident supersonic flow by the discharge, the flow temperature in the test section is measured using infrared emission spectroscopy. For this, a small amount of infrared active gas (2–4% of carbon monoxide) is added to the gas mixture. The rotational temperature of the flow is inferred from high-resolution CO infrared emission spectra taken with a Bruker Fourier transform infrared (FTIR) IFS-66 spectrometer. Each temperature measurement took about 30 s. Because of the relatively high flow density (about $\frac{1}{10}$ of the atmospheric density), the rotational and translational mode temperatures are in equilibrium.

III. Results and Discussion

Most experiments have been conducted in various N_2–He gas mixtures at the same plenum pressure of $P_0 = 250$ torr. The amount of nitrogen in the gas mixture was varied from 10 to 100%. The main reason for adding helium to the gas mixture was to lower the voltage required for sustaining the dc discharge ($U = 8$–12 kV in a 30% N_2–70% He mixture vs $U = 20$–25 kV in pure nitrogen), as well as to lower the power needed to sustain the rf discharge. However, both dc and rf discharges were equally diffuse and stable both in N_2–He mixtures and in pure nitrogen.

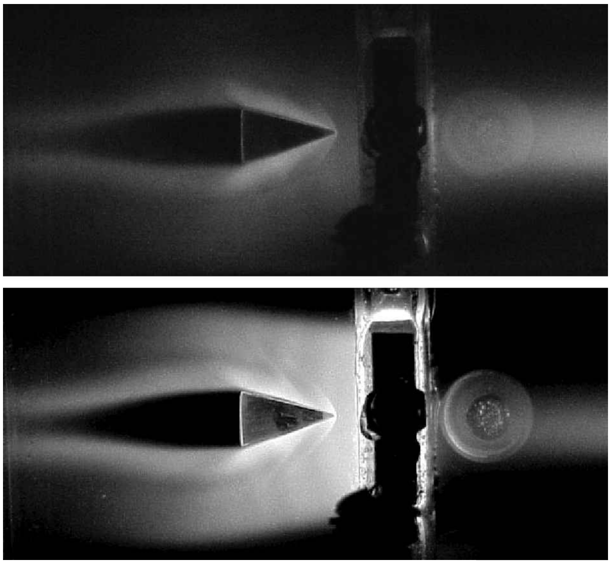

Fig. 2 Plasma flow visualization in a 50% N_2–50% He mixture: top, only dc discharge is on; and bottom, both dc and rf discharges are on.

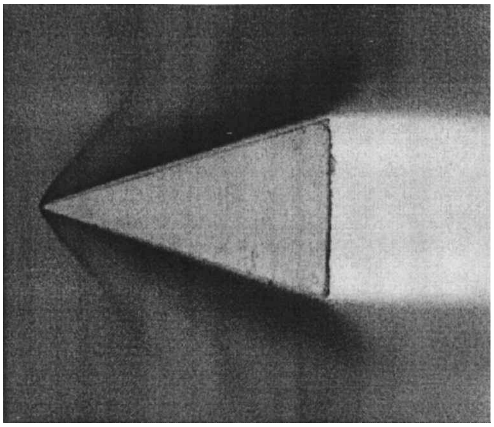

Fig. 3 Plasma flow visualization in a 50% N_2–50% He mixture: only dc discharge is on; wedge full angle is 35 deg, the shock full angle is 100 deg, which indicates Mach number of $M = 1.96$.

With the dc and/or rf discharge on, the nozzle, test section, and diffuser are filled with bright visible emission, arising primarily from the well-known second positive bands of nitrogen, $C^3\Pi_u \rightarrow B^3\Sigma_g$, and from the blue lines of helium.[9] Figure 2 shows typical color images of the flowfield around a 35-deg wedge in the test section in a 50% N_2–50% He mixture, with only the dc discharge on and both dc and rf discharges on. One can see that the visible emission makes all features of the supersonic flow, including shocks, boundary layers, expansion waves, and wakes, clearly visible. Detailed interpretation of the flow visualization mechanism is beyond the scope of the present paper; a brief discussion of the possible kinetic mechanisms involved can be found in Ref. 9. In addition to the primary oblique shocks, Fig. 2 also shows a pair of fainter secondary oblique shocks produced by the supersonic flow reflection off the boundary layer growing on the wedge walls, luminous boundary layers, centered expansion waves, where the supersonic flow turns a corner, and the dark wake behind the wedge. All of these features can be observed in real time simply by looking at the wind tunnel during its operation. Note that a slight curvature of the primary oblique shock near the nose of the wedge is due to a slight gap between the wedge and one of the nozzle walls, rather than the incident plasma flow nonuniformity. Indeed, Fig. 3 shows a high-resolution monochrome image of the test section flowfield in the same gas mixture but in a different nozzle with a much better fit between the wedge and the walls. One can see that in this case the oblique shock is nearly perfectly straight. The shock angle of $\alpha = 100$ deg indicates a test section Mach number of $M = 1.96$. In all experiments discussed in the present paper, the dc

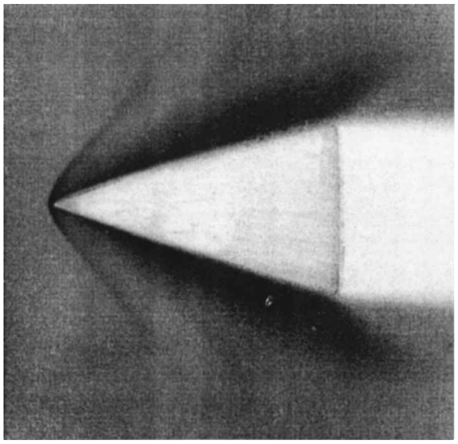

a) Only dc discharge on ($\alpha = 99$ deg)

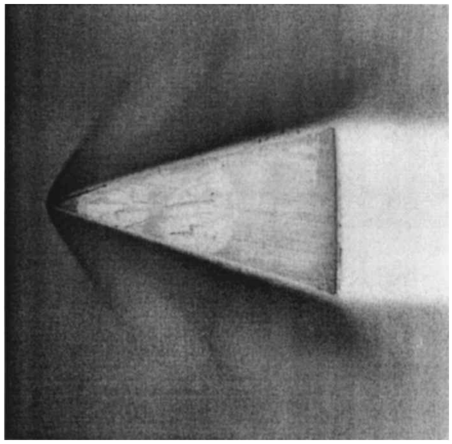

b) Both dc and rf discharges on ($\alpha = 113$ deg)

Fig. 4 Shock weakening by the plasma in a 30% N_2–70% He mixture.

discharge section used to produce a supersonic flowing afterglow is the same.

Turning the rf discharge on and off during the wind-tunnel operation resulted in a considerable shock angle increase. The dc discharge was on all of the time to provide plasma flow visualization and enable shock angle measurements with the rf discharge off. Figure 4 shows two high-resolution monochrome flow images in a 30% N_2–70% He mixture with the rf discharge on and off. In this experiment, the dc discharge voltage and current were 11 kV and 11 mA, respectively, so that the total dc power added to the flow is about 70 W (with about 50 W dissipated on a 400 KΩ ballast resistor). The rf discharge rms voltage and rms current were 1100 V and 180 mA, respectively, so that the total rf power was about 200 W. The electron density in the rf discharge, estimated from the rf current, is $n_e \cong 2 \times 10^{11}$ cm^{-3}, and the ionization fraction is $n_e/N \sim 10^{-7}$. From Fig. 4, one can see that the shock angle increases from $\alpha = 99$ to 113 deg, which corresponds to a flow Mach number reduction from $M = 2.0$ to 1.8. Figure 5 also shows a flow image composed of two separate frames, with the rf discharge on and off. Both frames have been differentiated using a Scion Image software package to highlight the location of the shock front and then added together. From Fig. 5, one can clearly see two shock fronts with distinctly different angles, the larger angle corresponding to the frame with the rf discharge on.

Using a COHU monochrome camera, we took a series of still flow frames during the run. The frames were taken at a frequency of approximately 1 frame/s. The objective was to look at the time-dependent behavior of the oblique shock with the rf discharge turned on and off. Figure 6 shows the oblique shock angle as a function of the frame number, that is, time. One can see that, after the rf discharge is turned on, the shock angle slowly (on the order of a few seconds) increases and reaches the near steady state. After the rf discharge is off, the reverse process, that is, shock angle recovery to

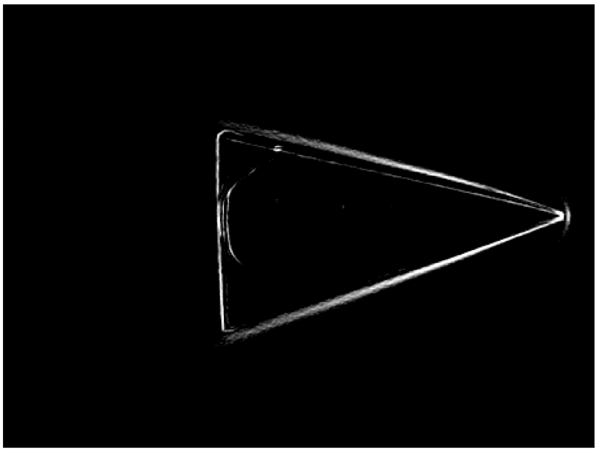

Fig. 5 Shock weakening by the plasma in a 30% N_2–70% He mixture; two flow images with rf discharge off and rf discharge on are differentiated to highlight the shock front location and then added together. The larger angle shock (117 deg) corresponds to rf on frame, and the smaller angle shock (105 deg) corresponds to the rf off frame.

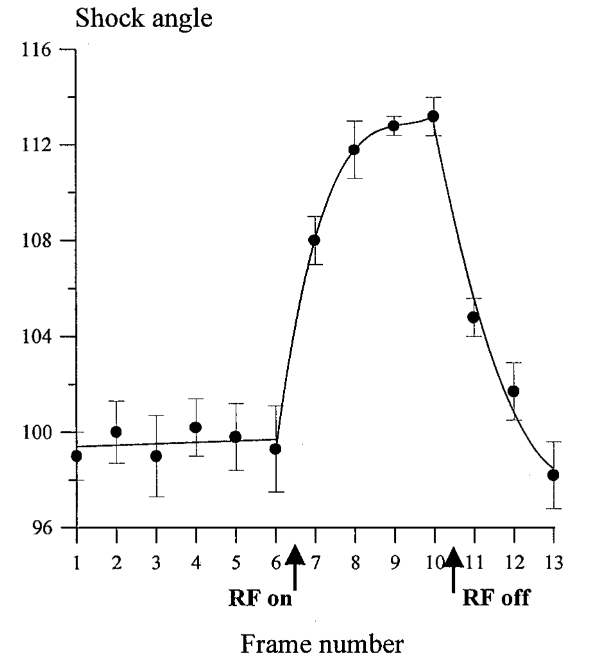

Fig. 6 Oblique shock angle as a function of a frame number, that is, time, in a 30% N_2–70% He mixture.

its initial value, also takes a few seconds. Note that the flow residence time in the test section is of the order of ten microseconds. During these experiments, both dc and rf voltage and current remained nearly constant in time.

The slow shock angle increase and recovery suggest a purely thermal mechanism, that is, the heating of the boundary layer in the third dimension (along the line of sight) and the nozzle walls near the rf discharge electrodes, which may well take a few seconds. The observed Mach number reduction is consistent with a flow temperature increase by $\Delta T = 24$ K. (This number is obtained for a one-dimensional Rayleigh flow at $M = 2$ with $\gamma = 1.55$.) In the present experiments, we never observed the anomalous shock behavior previously reported by several groups[1–5] (such as shock dispersion, shock splitting, and precursor formation in front of the shock). The shock front is always clearly defined, and no visible splitting occurs, for example, see Figs. 4 and 5. We believe that these previously reported effects are most likely to be due to nonuniform heating of the flow by the discharge, which in the present experiment is reduced to a minimum.

To determine whether the observed shock weakening is indeed a purely thermal effect, we measured the flow temperature in the test

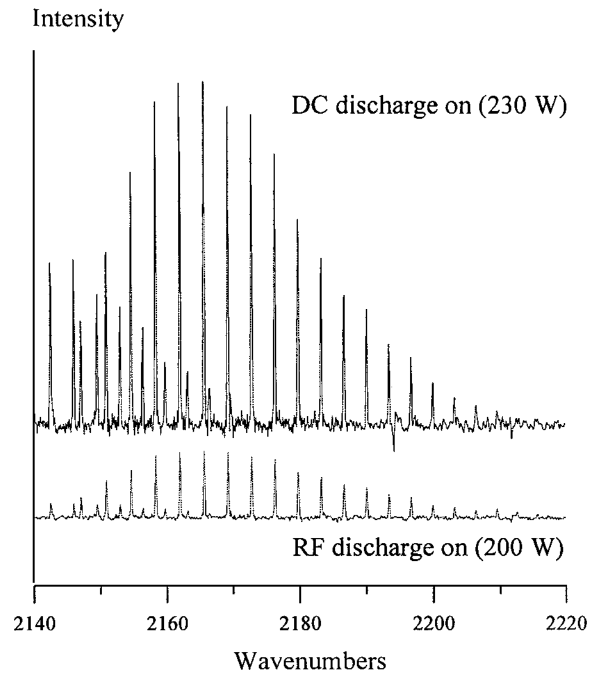

Fig. 7 Typical test section R-branch 1 → 0 CO emission spectra in a 75 torr N_2/175 torr He/10 torr CO mixture.

section, with only the dc discharge on, with only the rf discharge on, and with both discharges on, using infrared emission spectroscopy. For the temperature measurements, 10 torr of CO was added to the baseline 75 torr N_2/175 torr He mixture. The temperature was measured downstream of the rf electrodes but upstream of the wedge model, halfway between the nozzle axis and the wall. The FTIR signal was collected from a region of about 1 mm^2 area, while the rest of the nozzle was masked off. However, the resultant CO fundamental emission spectrum is integrated along the line of sight in the third dimension across the nozzle, which includes the boundary layers near the top and the bottom nozzle walls.

Figure 7 shows two typical CO fundamental emission spectra (R-branch of the $1 \rightarrow 0$ band) taken with only the dc discharge on and with only the rf discharge on. The dc discharge voltage and current were 19.6 kV and 24.0 mA, respectively, with about 230-W power added to the flow. The rf rms voltage and current were 1.6 kV and 120 mA, with the total rf power of about 200 W. Note that the measured CO $1 \rightarrow 0$ emission intensity in the dc discharge afterglow exceeds the emission intensity in the rf discharge afterglow by about a factor of five (Fig. 7). Also, the CO spectrum in the rf discharge afterglow has a very weak $2 \rightarrow 1$ band (a second series of rotational lines below 2170 cm^{-1}; Fig. 7). This shows that the CO vibrational temperature in the rf discharge is considerably lower than in the dc discharge. In other words, in the rf discharge a much smaller fraction of the input power goes into vibrational excitation, whereas more power goes into excitation of more rapidly relaxing electronic states of N_2 and He and ultimately into gas heating. This is consistent with the estimated reduced electric field values $(E/N)_{DC} \cong 5 \times 10^{-16}$ $V \cdot cm^2$ and $(E/N)_{RF} \cong 10 \times 10^{-16}$ $V \cdot cm^2$. Thus, the transverse rf discharge is expected to heat the gas flow more efficiently than the dc discharge.

Figure 8 shows Boltzmann plots obtained from two CO emission spectra, one with 230-W dc added to the flow, and the other with 230-W dc and 200-W rf coupled to the flow. One can see that in both cases the flow is optically thin for the CO emission because there is no significant self-absorption among the low rotational levels. The best fit to the data obtained using the rotational maxima between $J' = 1$ and $J' = 12$ corresponds to the translational–rotational temperatures of $T = 190$ and 221 K for these two cases. However, the best fit to the rotational maxima from $J' = 13$ and $J' = 19$ gives the temperatures of $T = 200$ and 271 K, respectively. This result most likely indicates a temperature nonuniformity across the line of sight, with the lower temperature in the inviscid core and the higher recovery temperature in the boundary layer.

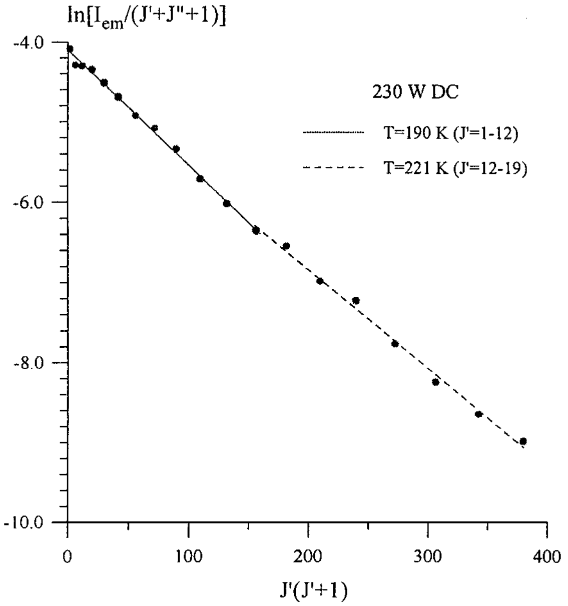

a) **Only dc discharge on**

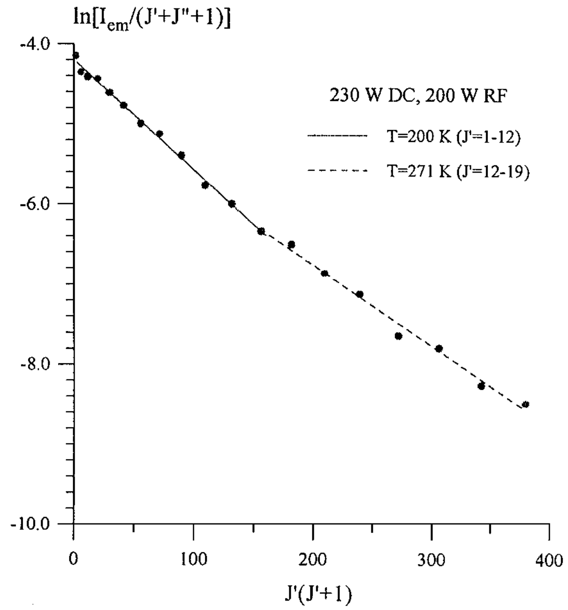

b) **Both dc and rf discharges on**

Fig. 8 Boltzmann plots of the CO emission spectra in a 75 torr N_2/175 torr He/10 torr CO mixture.

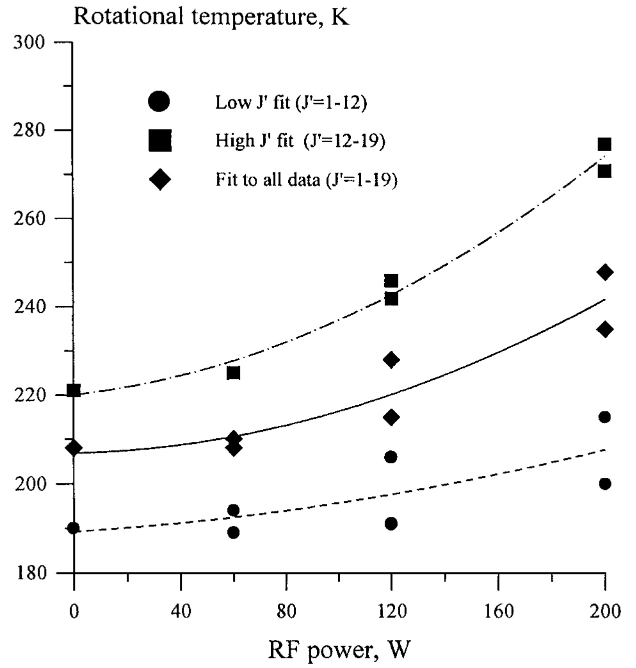

Fig. 9 Test section temperature in a 75 torr N_2/175 torr He/10 torr CO mixture as a function of the rf discharge power; at each value of rf power, the temperature is measured both with the 230-W dc discharge on and off.

a)
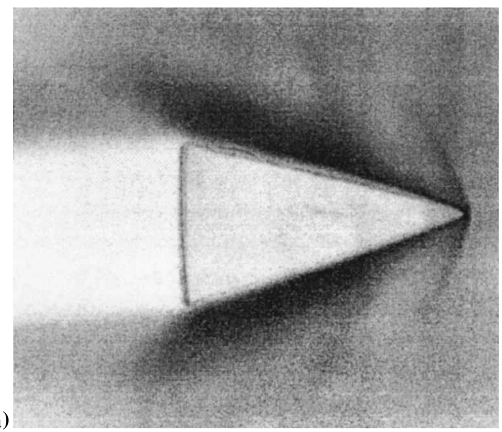

b)
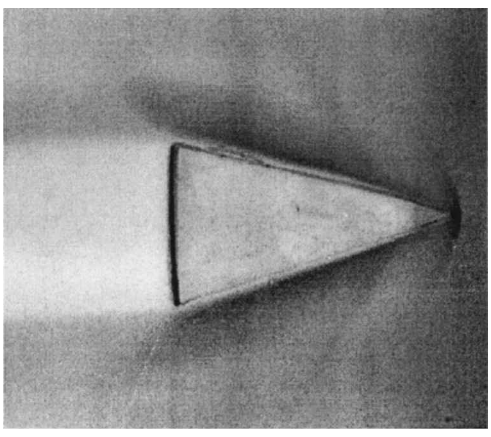

Fig. 10 Oblique shock and bow shock in a 10% N_2/90% He mixture: a) rf discharge off and b) rf discharge on. Shock standoff distance increase is 0.1 mm.

Figure 9 shows the flow temperature as a function of the rf discharge power added to the flow. At each value of the rf power, the temperature was measured both with the 230-W dc discharge on and off. One can see that when 200-W rf power is added to the flow, the temperature inferred from the low rotational level populations ($J' = 1$–12) increases by only $\Delta T = 15$ K, whereas the temperature inferred from the high rotational levels populations ($J' = 12$–19) rises by $\Delta T = 50$ K. The temperature inferred from all available data ($J' = 1$–19) increases by $\Delta T = 35$ K. This can be interpreted as preferential heating of the boundary layers by the rf discharge. This temperature increase is consistent with the one-dimensional estimate of the temperature rise needed to explain the observed shock angle change by the flow heating, $\Delta T = 24$ K. Thus, the temperature measurements, in addition with the extremely slow shock weakening and recovery (see Fig. 6), suggest that the shock control by the plasma is a purely thermal effect.

The emission spectroscopy measurements also explain why the use of 200-W rf power results in a substantial shock weakening, whereas adding 500 W of dc power to the flow does not produce any detectable effect on the shock angle.[9] Basically, it occurs because in

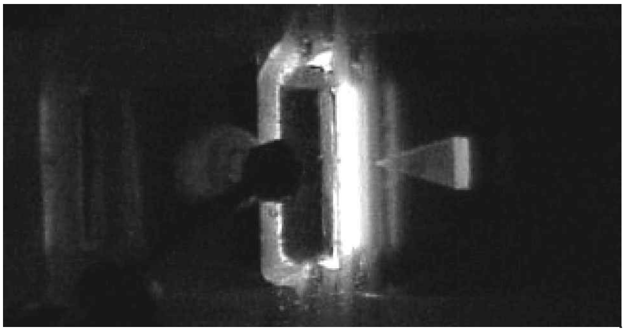

Fig. 11 Transverse rf discharge in atmospheric air; P_0 = 250 torr.

the transverse rf discharge a larger fraction of the electric field power goes to gas heating, which preferentially occurs in the boundary layers.

An additional run was conducted in a 10% N_2/90% He mixture. In flows with large fraction of helium, the oblique attached shock becomes strongly curved and closely resembles a bow shock. With both 30-W dc discharge and 100-W rf discharge turned on, the shock standoff distance increased by about 0.1 mm (Fig. 10).

In the last series of experiments, the nonequilibrium plasma wind-tunnel facility was operated in atmospheric air. Room air entered the nozzle plenum at the pressure $P_0 = 250$ torr through a valve opened in the gas line upstream, and the transverse rf discharge was initiated in the supersonic test section. As in all earlier runs in N_2–He mixtures and in nitrogen, the discharge in air was diffuse and stable, with no sign of arc filaments (Fig. 11). The only significant difference from the N_2–He runs was that the visible afterglow in air was nearly absent due to very rapid relaxation of radiating electronically excited molecules, which did not allow straightforward plasma flow visualization. For this reason, no plasma shock weakening measurements in air have been performed. However, such measurements can be easily made on the present facility using a conventional schlieren system available in our group. These experiments showed that uniform and stable plasma with the electron density of $n_e = 3 \times 10^{11}$ cm^{-3} can be sustained in supersonic airflows using a transverse rf discharge. Both electron density and ionization efficiency are expected to be considerably increased by replacing the sine wave rf voltage by a series of very short high-voltage pulses, such as been done in high-power CO lasers.[12] This would allow operation at a very low duty cycle and would, therefore, greatly improve the discharge stability and the plasma power budget,[12] thereby opening a possibility of the use of transverse high-frequency pulsed discharges for magnetohydrodynamic (MHD) energy extraction and/or acceleration of supersonic airflows.[13,14] The high-voltage, high repetition rate pulsed power supply for this application is currently being developed at Ohio State University.

IV. Summary

A unique supersonic nonequilibrium plasma wind tunnel, which produces a highly nonequilibrium plasma flow with low gas kinetic temperatures at $M = 2$, is used for studies of shock modification by nonequilibrium plasmas. Supersonic flow is maintained at complete steady state. The flow is ionized by a high-pressure aerodynamically stabilized dc discharge in the tunnel plenum and by a transverse rf discharge in the supersonic test section. The dc discharge is primarily used for the supersonic flow visualization, whereas the rf discharge provides high electron density for shock modification in the supersonic test section. High-pressure flow visualization produced by the plasma makes all features of the supersonic flow, including shocks, boundary layers, expansion waves, and wakes, clearly visible. Attached oblique shock structure on the nose of a 30-deg wedge with and without rf ionization in a $M = 2$ flow is studied in various nitrogen–helium mixtures. It is found that the use of the rf discharge increases the shock angle by 14 deg, from 99 to 113 deg, which corresponds to Mach number reduction from $M = 2.0$ to 1.8. Time-dependent measurements of the oblique shock angle show that the time for the shock weakening by the plasma, as well as the shock recovery time after the plasma is turned off, is of the order of seconds. Because the flow residence time in the test section is of the order of 10 μs, this result suggests a purely thermal mechanism of shock weakening due to heating of the boundary layers and the nozzle walls by the discharge. Gas flow temperature measurements in the test section using infrared emission spectroscopy, with carbon monoxide as a thermometric element, are consistent with the observed shock angle change. This also shows that shock weakening by the plasma is a purely thermal effect. The results demonstrate feasibility of both sustaining uniform ionization, with electron density up to $n_e = 3 \times 10^{11}$ cm^{-3} in supersonic nitrogen and airflows and the use of nonequilibrium plasmas for supersonic flow control. This opens a possibility for the use of transverse stable rf discharges for nonequilibrium MHD energy extraction and/or acceleration of supersonic airflows.

Acknowledgments

The support of MSE Technologies, Inc., under a NASA prime, and the Air Force Office of Scientific Research is gratefully acknowledged. Partial support from the Ohio Board of Regents Investment Fund is gratefully acknowledged. We would also like to express our sincere gratitude to Frank DeLucia and Scott Harris for useful suggestions and to Mo Samimy for lending us a digital color camera.

References

[1]Klimov, A. I., Koblov, A. N., Mishin, G. I., Serov, Y. L., and Yavor, I. P., "Shock Wave Propagation in a Glow Discharge," *Soviet Technical Physics Letters*, Vol. 8, No. 4, 1982, pp. 192–194.

[2]Basargin, I. V., and Mishin, G. I., "Probe Studies of Shock Waves in the Plasma of a Transverse Glow Discharge," *Soviet Technical Physics Letters*, Vol. 11, No. 11, 1985, pp. 535–538.

[3]Mishin, G. I., Klimov, A. I., and Gridin, A. Y., "Measurements of the Pressure and Density in Shock Waves in a Gas Discharge Plasma," *Soviet Technical Physics Letters*, Vol. 17, No. 8, 1991, pp. 602–604.

[4]Ganguly, B. N., Bletzinger, P., and Garscadden, A., "Shock Wave Damping and Dispersion in Nonequilibrium Low Pressure Argon Plasmas," *Physics Letters A*, Vol. A230, 1997, pp. 218–222.

[5]Lowry, H., Stepanek, C., Crosswy, L., Sherrouse, P., Smith, M., Price, L., Ruyten, W., and Felderman, J., "Shock Structure of a Spherical Projectile in Weakly Ionized Air," AIAA Paper 99-0600, 1999.

[6]Adamovich, I. V., Subramaniam, V. V., Rich, J. W., and Macheret, S. O., "Phenomenological Analysis of Shock Wave Propagation in Weakly Ionized Plasmas," *AIAA Journal*, Vol. 36, No. 5, 1998, pp. 816–822.

[7]Ionikh, Y. Z., Chernysheva, N. V., Yalin, A. P., Macheret, S. O., Martinelli, L., and Miles, R. B., "Shock Wave Propagation Through Glow Discharge Plasmas: Evidence of Thermal Mechanism of Shock Dispersion," AIAA Paper 2000-0714, 2000.

[8]Macheret, S. O., Martinelli, L., and Miles, R. B., "Shock Wave Propagation and Structure in Non-Uniform Gases and Plasmas," AIAA Paper 99-0598, 1999.

[9]Yano, R., Contini, V., Plönjes, E., Palm, P., Merriman, S., Aithal, S., Adamovich, I., Lempert, W., Subramaniam, V., and Rich, J. W., "Supersonic Nonequilibrium Plasma Wind-Tunnel Measurements of Shock Modification and Flow Visualization," *AIAA Journal*, Vol. 38, No. 10, 2000, pp. 1879–1888.

[10]Raizer, Y. P., *Gas Discharge Physics*, Springer, Berlin, 1991, Chaps. 5, 13.

[11]Raizer, Y. P., Shneider, M. N., and Yatsenko, N. A., *Radio-Frequency Capacitive Discharges*, CRC Press, Boca Raton, FL, 1995, Chap. 1.

[12]Generalov, N. A., Zimakov, V. P., Kosynkin, V. D., Raizer, Y. P., and Roitenburg, D. I., "Method for Significantly Increasing the Stability Limit of the Discharge in Fast-Flow Large-Volume Lasers," *Technical Physics Letters*, Vol. 1, 1975, p. 431.

[13]Macheret, S. O., Shneider, M. N., Miles, R. B., Lipinski, R. L., and Nelson, G. L., "MHD Acceleration of Supersonic Air Flows Using Electron Beam Enhanced Conductivity," AIAA Paper 98-2922, June 1998.

[14]Macheret, S. O., Shneider, M. N., and Miles, R. B., "MHD Power Extraction from Cold Hypersonic Air Flow with External Ionizers," AIAA Paper 99-4800, 1999.

M. Sichel
Associate Editor